CHAPTER III

THEORY

To well understand the nature of coke deposited on the catalysts, one needs some backgrounds of deactivation by coking. In this chapter, some basic information of coke concerning is briefly described which will help in understanding the nature of coke from specific reaction and deposition. Three sections are involved: Effects of carbon deposits on the dehydrogenation reaction, Composition, Structure and Localization of Carbon Deposits, and Coke formation kinetics. As mentioned earlier, BET surface area measurement and pore size distribution are the essential method in the present work, so that the developed common method is mentioned later in this chapter.

3.1 Catalyst Deactivation

A catalyst may lose its activity or its selectivity for a wide variety of reasons. The causes may be grouped loosely into (Satterfield, 1980)

1. Poison
2. Fouling
3. Reduction of active area by sintering or migration
4. Loss of active species

One of these deactivation which was mainly focused on the present work is the deactivation by fouling. The term fouling is generally used to describe a physical blockage such as the deposit of dust of fine powder or carbonaceous deposits (coke). In the latter case activity can usually be restored by removal of the coke by burning.

The deactivation by fouling have been paid attention by many researchers for a long times. Hughes (1984) has mentioned that the catalyst deactivation by fouling usually involves significant amounts of deposits material. Amount up to 10-20 % of the catalyst weight were frequently obtained. Basically, two types of fouling may occur, due to (1) the reaction system itself and (2) deposition by an impurity in the feed stream.

The first is typified by "coke" or carbon deposition on catalysts which occurs under certain conditions when hydrocarbon streams are processed. Since the deposit originates from a cracking type reaction either in the feed stream or in the various products, it can not be completely eliminated. On the other hand, the latter is typified by poisoning so that the feed may , in principle, be purified to remove the impurities.

The fouling by coke deposition is always associated with the main reaction. Therefore, it is usually not possible to eliminate the coke deposition totally, but the process of coking can often be substantially reduced by modifying the catalyst so as to improve its selectivity. An example of this is the addition of small amounts of alkali to steam reforming catalysts. This reduces the acidity of the catalyst and tends to reduce the cracking type reactions that may occur.

Examples of reactions that produce carbonaceous deposits are extremely numerous. Virtually any process having carbon atoms in the feed or product molecules can, under appropriate conditions, gives rise to deposition of coke. Naturally, molecules with large numbers of carbon atoms and/or those with aromatic or naphthenic rings tend to produce coke deposits more easily. Both aromatics and olefins are the immediate coke precursors which readily yield coke deposits.

Butt (1988) has also stated on the deactivation by fouling that the strongly adsorbed carbonaceous deposits form large polynuclear aromatic structures, apparently through polymerization and condensation. However, coke is not a well-defined

substance; normally it has an empirical formula approximating CH, but the chemical nature depends very much on how it is formed. For example, coke is known to develop in filamentous or whisker-like structures or encapsulating-type structures on metals and in pyrolytic-type structures on acidic surfaces. The coke also varies depending on the conditions of temperature and pressure. Moreover, these structures change as they age on the catalyst surface. Thus, it is apparent that there are great variations in the morphology of the coke depending on the catalyst and its history. Butt (1988) has commented that industrial hydrocarbon feeds are complex mixtures of compounds and the amount and type of coke formed depend on the chemical nature of the feed and products formed. The activity of the catalyst depends on the number of active centers that are available to carry out the main reactions.

Hughes (1984) has noted that coking would occur in a reaction either in parallel or consecutive to the main reaction. This coke profile would be descending in the case of a parallel mechanism but ascending for a consecutive (or series) mechanism. The parallel and consecutive reactions for coking can be written as follows:

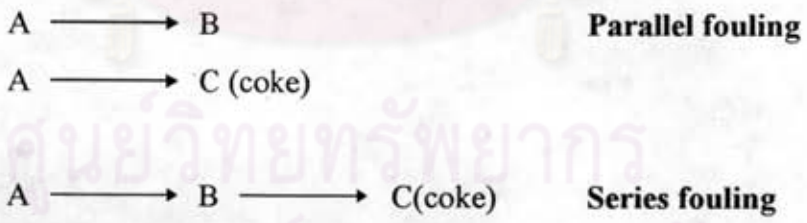

Thus, parallel fouling gives large coke deposits when the reactant concentration is high, since the reactant is the coke precursor. Therefore, when coking occurs by a parallel mechanism, the greatest deposition of coke would be expected at the inlet of the reactor. Conversely, larger coke deposits are formed in series fouling, when the product B has a high concentration since this is the immediate precursor of the coke in this case. In normal operation the product concentration increases with distance along the reactor, and therefore the coke distribution should follow a similar pattern.

3.2 Effects of Carbon Deposits on the Dehydrogenation Reaction

Franck and Martino (1985) observed the effect of carbon deposits on the main reforming reactions: dehydrogenation, dehydroisomerization, isomerization, and dehydrocyclization.

Dehydrogenation of paraffins and naphthenes is a fast reaction, and, under reforming conditions, the corresponding thermodynamic equilibria are rather quickly achieved. The olefin concentrations that may be formed therefore remain quite low, so the dehydrogenation of cyclohexanic naphthenes are considered here.

For low carbon coverage at atmospheric pressure, about three carbon atoms are needed to suppress dehydrogenating activity of two Pt atoms. The results given in figure 3.1 were obtained by treating a cyclohexane-toluene mixture (20 % cyclohexane by weight) on previously coked reforming catalysts (0.6% Pt by weight) at 300°C under atmospheric pressure. It was seen that activity, expressed in moles of benzene obtained per gram of catalyst per hour, dropped very quickly when the carbon content increased. On the other hand, according to these results, the activity of the catalyst should be nil with a coke content on the order of 0.1 wt. % if all the carbon was deposited on the platinum. The results in figure 3.1 show that , in fact, most of the carbon was found on the alumina.

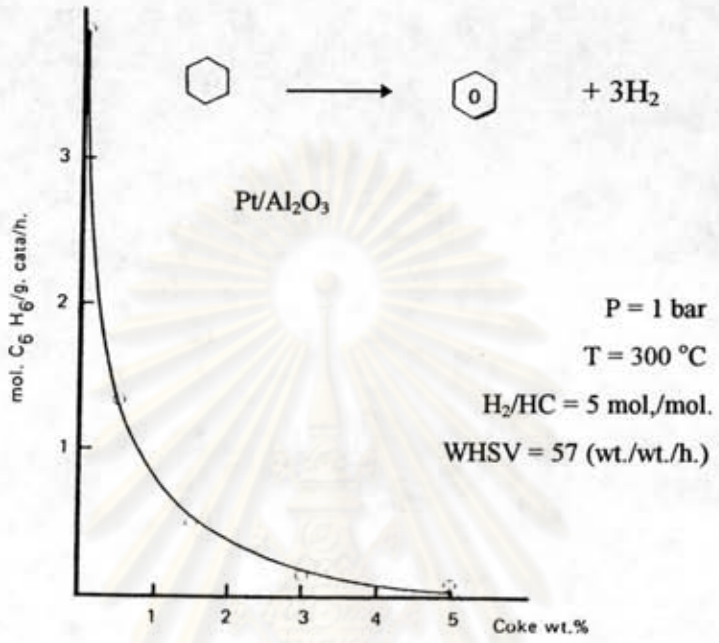

Figure 3.1 Effect of coke on dehydrogenation activity. (Franck and Martino, 1985)

3.3 Composition, Structure, and Location of Carbon Deposits

3.3.1. Composition

Franck and Martino (1985) stated that carbon deposits are formed from hydrocarbons which almost never have more than 12 carbon atoms and usually have fewer than 10. On the average, a naphtha treated in reforming has at least two hydrogen atoms for each carbon atom, and if recycled hydrogen is taken into account, the hydrogen/carbon atomic ratio in the reactive phase is between 3 and 4. The combined feedstock of naphtha plus recycle gas is therefore rich in hydrogen when compared with various hydrocarbons (methane,paraffins, or aromatics), with different petroleum cuts, and especially with crude oils or coals, as shown in Table 3.1.

Table 3.1 H/C Ratio of Various Hydrocarbons, Petroleum Cuts, Coal Liquids, and Coals

Compound	H/C (wt %)	H/C (atomic)
CH_4	0.33	4.0
Paraffins	0.17	2.0
Benzene	0.083	1.0
Naphthalene	0.067	0.8
Straight-run naphtha	0.16	1.9
Coal liquid naphtha	0.13	1.56
Crude oil	0.09-0.13	1.08-1.56
Syncrude	0.07-0.10	0.84-1.20
Coal	0.05-0.07	0.60-0.84
Reformer combined feed	0.22-0.366	2.64-4.32

[a]Naphtha + hydrogen with $3 < H_2/HC < 10$

They remarked about techniques for determining carbon and hydrogen composition. The consolidated carbon deposits may occur when the coke are determined after stripping at high temperature. On the other hand, the coke which are more or less mobile, formed by the heavy aromatic hydrocarbons which are always present under operating conditions and which remain adsorbed on the catalyst when the catalytic bed is cooled down. They therefore distinguished between deposits whose concentration can be determined by combustion after having taken the necessary precautions and those, on the other hand, which are precursors of such deposits and whose presence can be determined either by kinetic methods or by means of extraction using solvents.

Table 3.2 shows a few H/C ratios measured for different carbon deposits; it may be noted that the data concerning reforming are rather rare. In the case of cracking or dehydrogenation reactions occurring without hydrogen, the figures are low, usually lower than those obtained for most coals. As far as reforming is concerned, the two figures given are very different: The first is an average of a few hundred results obtained on industrial samples treated for 24 hr at 100°C , while the second was obtained after various solvent extraction treatments and high-temperature calcination, which probably left only the most refractory of those deposits on the catalyst. These differences show that even the carbon deposits which are called "consolidated" can be partially dissolved, which admit that there is, on the surface of the catalyst, a very wide spectrum of "carbon deposits," from those which are still soluble to products which are very close to inertinite.

As far as "mobile deposits" are concerned, it has been possible to detect unnegligible amounts of heavy hydrocarbons, under special conditions, in reforming effluents both from n-heptane and from butylbenzene or from a real feedstock. They concluded that the deposits found on coked catalysts can be

anything from polyaromatic hydrocarbons to coals which cannot be dissolved in organic solvents.

Table 3.2 H/C Ratio (wt. %) of Coke Deposits Obtained in Various Processes

Process	Feed	Catalysts	H/C
Cat-cracking	Midcontinent G.O.	SiO_2/Al_2O_3	0.03-0.04
Dehydrogenation	Isopentane	Cr_2O_3/Al_2O_3	0.005-0.013
Cat-cracking	Aromatics	SiO_2-Al_2O_3	0.03-0.07
Cat-reforming	Straight-run naphtha	Pt/Al_2O_3	0.05-0.10[a]
Cat-reforming	Pure hydrocarbons	Pt/Al_2O_3	< 0.01[b]

[a] Measured after stripping with air during 24 hr at 110°C and removal of adsorbed water.

[b] Measured after washing with C_2H_5OH-C_6H_6, dissolution of alumina, and air treatment at 110°C

3.3.2. Structure

Franck and Martino (1985) assumed that the carbon deposits are uniformly spread out on the surface of the catalyst. In the case of reforming catalyst, specific area 200m^2/g, there would be a carbon monolayer for consolidated coke concentrations on the order of 10 wt %. Observations made during catalytic cracking show that rather large aggregates are involved. These aggregators have, moreover, been studied with different techniques, such as thermal analysis, X-rays, electron microscopy, and various kinds of spectroscopy (infrared and Auger). However, some detailed characterizations of deposits obtained in reforming still remain relatively rare; in Espinat's study, different techniques were used and compared for characterizing carbon deposits on reforming catalysts.

X-ray diffraction

The use of x-ray diffraction for characterizing carbon deposits on a used catalyst has made it possible to show the presence of three-dimensional aggregates which are well crystallized. However, in order to have a more sensitive analysis, the alumina is previously dissolved with hydrofluoric acid, and an x-ray diffraction spectrum such as the one shown in figure 3.2 is thus obtained. Curve I shows that the band corresponding to grahpite (002) is very intense, whereas the other bands are not so clearly defineq. By increasing the counting time (curve II), it has been possible to improve the resolution of bands (101) and (100), bands (102) and (004), as well as band (110).

They found that the coke particle measures about 4.5 nm along axis (002), which corresponds to a stacking of about a dozen graphitic planes. In the same way, following axis (101), a size of about 2.0 nm was found, in other words, when d = 2.09°A, about 10 planes. These results confirm that this graphitic coke represents only a fraction of the total amount of coke and that its structure depends on the compounds treated during coking.

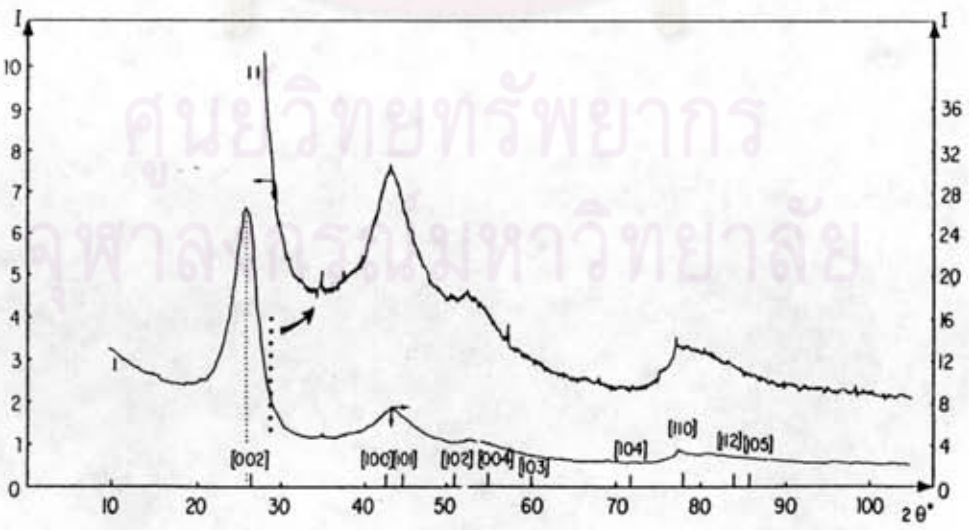

Figure 3.2 X-ray pattern of coke deposit.

Raman spectroscopy

In Espinet's study, alongside a fluorescence related to the presence of nondesorbed heavy polyaromatic hydrocarbons, two intense bands are detected on the coked catalysts in the region 1300-1650 cm^{-1}, and these are characteristic of graphitic carbons. This technique, which as the advantage of being applicable even with low percentages of coke, has made it possible to demonstrate that, with 0.3 wt % carbon, coke are already organized structures, thus proving that the formation of localized carbonaceous aggregates takes place from the very beginning of the reaction.

3.3.3. Location

Concentration in the grain

Scanning microprobe studies of catalysts coked under conditions approximating industrial operation reveal that the coke is distributed homogeneously in the catalyst grain: concentrations on the periphery and in the core of the grain are completely comparable.

Closer analysis by ionic microprobe confirms this overall homogeneous distribution, with, however, variations in local concentration of 0.5-2.7 wt % for an average coke content of 1.15 % as shown in fig.3.3. For reference purposes, this figure also contains recording of the alumina, platinum, and chlorine signals.

Local concentration

By use of electron microscopy, it is possible to localize the coke on the micrograin level. Thus it was noted that alongside clearly organized

aggregates, there do exist zones which are little coked. Furthermore, spectroscopic analysis of electron energy loss shows that alongside zones which are rich in well-organized coke, there are zones which are just as rich but in which the coke has an amorphous structure.

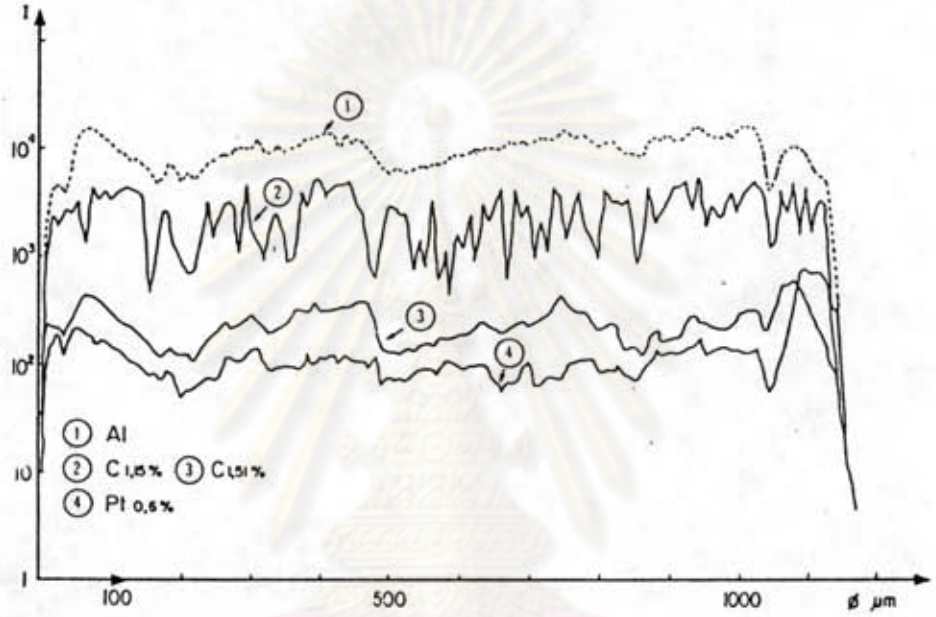

Figure 3.3 Ionic microprobe analysis of a coked catalyst (Franck and Martino 1985)

The formation of three-dimensional carbonaceous aggregates, whatever their structure might be, logically leads us to suppose that the alumina pores are blocked. The results given in fig.3.4 show that whereas the total porous volume decreases linearly according to carbon content, the BET surface area diminishes very quickly with the first few percent of carbon, and much more slowly thereafter. These observations correspond to rapid plugging of the smallest pores, even with very low coke concentrations.

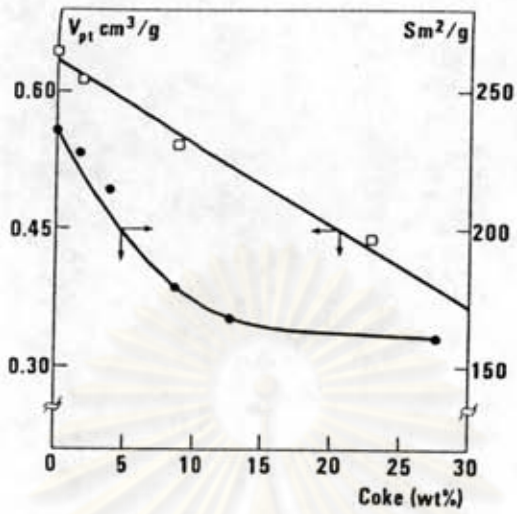

Figure 3.4 Effect of coke deposit on specific area and pore volume. (Franck and Martino 1985)

3.4 Coke Formation Kinetics

Kinetics models of fouling used to describe catalyst decay were presented by Wejciechowski and Corma (1986). Two approaches have been used to describe decay. One is based directly on measurement of coke on catalyst (COC) and the other is based on time on stream (TOS).These two have been, more successful in dealing with real systems.

3.4.1. Decay Models Based on Coke on Catalyst

Kinetic models of catalyst decay based on COC are attractive in the first instance because they seem to relate loss of activity to the amount of supposed deactivating agent. Unfortunately, the variety of coke origins and the range of mechanisms by which coke can cause deactivation make modeling by this approach very cumbersome, both experimentally and mathematically.

The major effort in developing the COC approach has been that of Froment (1985), who, in deriving his kinetic descriptions of catalyst decay, has had to make significant simplifications of the complex reality in the decay phenomena. The result is that this treatment describes coke deposition and catalyst activity using empirical concepts. Froment defined a_A as the "activity" of the catalyst with respect to the main cracking reaction and a_C as the activity with respect to coke-producing reactions. He then related these activities to the fraction of sites available for reaction:

$$a_A = \left(\frac{C_t - C_{cl}}{C_t}\right)^{n_A} \tag{3.1}$$

$$a_C = \left(\frac{C_t - C_{cl}}{C_t}\right)^{n_C} \tag{3.2}$$

where C_t is the total concentration of sites available for reaction and C_{cl} is the concentration of poisoned sites. Equation 3.1 and 3.2 express a model rather than any

mechanistic reality and in practice can be replaced by any suitable modeling function that leads to a good fit of a given data set. For example, the functions

$$a_A = \exp(-\alpha_A C_c) \tag{3.3}$$

$$a_C = \exp(-\alpha_c C_c) \tag{3.4}$$

allow a connection to be made between the activities and C_c, the coke on catalyst. Defining "activities" in this way leads to rate expressions of the form

$$\frac{dC_X}{dt} = r_X^o \, a_A \tag{3.5}$$

$$\frac{dC_C}{dt} = r_C^o \, a_C \tag{3.6}$$

where C_X = fraction of the feed converted

C_C = coke on catalyst

$r_{X,C}^o$ = rate of the respective reactions at zero coke level

t = time on stream

Introducing Equations (3.3) and (3.4) into (3.5) and (3.6) and integrating, one obtains

$$C_x = \frac{1}{\alpha_A} \ln\left(1 + \alpha_A r_X^o t\right) \tag{3.7}$$

$$Cc = \frac{1}{\alpha_C} \ln\left(1 + \alpha_C r_C^o t\right) \tag{3.8}$$

Equations (3.7) and (3.8) are clearly a long way from the initially hoped for mechanistic model of the effects of coke on catalyst activity. They can be fitted to experimental data to yield α_A ,α_C , r_X^o, and r_C^o and hence can be used to describe coke profiles and activity behavior.

They commented that the complex nature of coke does not allow a more mechanistic interpretation of catalyst decay. Furthermore, coke measurements are time consuming and subject to experimental error, making the use of COC models of catalyst decay cumbersome to use in practice.

All in all, the advantages of COC models that were anticipated have not materialized in practice. Nevertheless, the methods of Froment are a valuable source of correlation for describing coke-on-catalyst profiles in reactors.

3.4.2. Decay Models Based on Time on Stream

The difficulties described in Section 1 with respect to achieving a mechanistic model of catalyst decay are such that many workers have resorted to the much more convenient and less mechanistic functional dependence of catalyst activity on time on stream. Perhaps the simplest such model involves the assumption that catalyst activity **"a"** is linearly dependent on the time on stream **t** :

$$a = a_o - At \tag{3.9}$$

whose differential form is zero order in activity.

$$-\frac{da}{dt} = A \tag{3.10}$$

More elaborate forms use first-order dependencies,

$$-\frac{da}{dt} = Aa \tag{3.11}$$

$$a = a_o \exp(-At) \tag{3.12}$$

second-order dependencies,

$$-\frac{da}{dt} = Aa^2 \tag{3.13}$$

$$\frac{1}{a} = \frac{1}{a_0} + At \tag{3.14}$$

and other more involved forms, such as those used by Blanding(1953) and Voorhies (1945)

$$-\frac{da}{dt} = BA^{1/2}a^{(B+1)/B} \tag{3.15}$$

$$\left(\frac{1}{a}\right)^{1/B} = \text{const}_1 + \text{const}_2(t) \tag{3.16}$$

All these forms were applied successfully in specific cases. In particular, the exponential form given in Equation (3.12) allowed to develop models of catalytic cracking which were mathematically and esthetically pleasing in their simplicity.

All the decay functions above can be encompassed by the generalized forms developed in the time-on-stream theory, where it is postulated that the "activity" is in fact directly related to the concentration of active sites, C_s, on the catalyst. An expression for the dependence of C_s is as follow:

$$-\frac{dC_S}{dt} = k'_{0d} + k'_{1d}C_S + k'_{2d}C_S^2 + \ldots\ldots + k'_{md}C_S^m \qquad (3.17)$$

In Equation (3.17) the various modes of decay due to site poisoning, diffusion, and so on, are approximated by the various power-law terms in the series, and it is assumed that the several decay reactions proceed in parallel.

The major simplifying assumption in Equation (3.17) is the implicit assumption that decay is not a function of reactant or product concentration. This is obviously impossible in practice, except in the case where the reactants and products are equally poisonous to the catalyst and both conversion and decay are first order. However, even in much more complex cases, the time-on-stream function derived from Equation (3.17) describes the observed results very well. The reasons for this are, first, that in practice both reactants and products do contribute significantly to coke formation , and second, that Equation (3.17) reduces to a very flexible form on further analysis.

Rewriting Equation (3.17) in terms of $\theta = C_s/C_{sO}$, the fraction of sites still active.

$$-\frac{d\theta}{dt} = k_{0d} + k_{1d}\theta + k_{2d}\theta^2 + \ldots\ldots + k_{md}\theta^m \qquad (3.18)$$

where $k_{md} = k'_{md}C_{so}^{m-1}$. It has been shown that Equation (3.18) is very well represented by the simpler equation

$$-\frac{d\theta}{dt} = k_d\theta^m \qquad (3.19)$$

if the exponent **m** is allowed to assume nonintegral values. In fact, Equation (3.19) fits data fitted by all the various time-on-stream equations(3.9) to (3.16) and provides a broadly applicable functional description of catalyst decay.

On integration of Equation (3.19), one obtain

$$\theta = \left(\frac{1}{1+Gt}\right)^{N} \qquad m \neq 1 \qquad (3.20)$$

where $G = (m-1)k_d t$ and $N = 1/(m-1)$.

The functional form shown in Equation (3.20) has been successfully applied to a great variety of cracking and dehydrogenation reactions and has been the basis of a considerable improvement in understanding the behavior of cracking catalysts. In particular, it has allowed an improved understanding of selectivity behavior on rapidly decaying catalysts.

3.5 Brunauer-Emmett-Teller (BET) Method.

The most common method of measuring surface area, and one used routinely in most catalyst studies, is that developed by Brunauer, Emmett, and Teller (1938). Early descriptions and evaluations are given by Emmett (1948, 1954). In essence, the Langmuir adsorption isotherm is extended to multilayer adsorption. As in the Langmuir approach, for the first layer the rate of evaporation is considered to be equal to the rate of condensation, and the heat of adsorption is taken to be independent of coverage. For layers beyond the first, the rate of adsorption is taken to be proportional to the fraction of the lower layer still vacant. The rate of desorption is taken to be proportional to the amount present in that layer. The heat of adsorption for all layers except the first layer is assumed to be equal to the heat of liquefraction of the adsorbed gas. Summation over an infinite number of adsorbed layers gives the final expression as follows:

$$\frac{P}{V(P_o - P)} = \frac{1}{V_m C} + \frac{(C-1)P}{V_m C P_o} \qquad (3.21)$$

where V= volume of gas adsorbed at pressure P

V_m = volume of gas adsorbed in monolayer, same units as V

P_o = saturation pressure of adsorbate gas at the experimental temperature

C = a constant related exponentially to the heats of adsorption and liquefraction of the gas

$$C = e^{(q1 - qL)/RT} \qquad (3.22)$$

where q_1 = heat of adsorption on the first layer

q_L = heat of liquefraction of adsorbed gas on all other layers

The larger the value of C the more the isotherm approaches the type II form and the more accurately the surface area can be determined.

If Eq. (3.21) is obeyed, a graph of $\frac{P}{V(P_o - P)}$ versus P/P_o should give a straight line whose slope and intercept can be used to evaluate V_m and C. Many adsorption data show very good agreement with the BET equation over values of the relative pressure P/P_o between approximately 0.05 and 0.3, and this range is usually used for surface-area measurements. At higher P/P_o values, complexities associated with the realities of multilayer adsorption and/or pore condensation cause increasing deviation. At values of P/P_o much below about 0.05 the amount adsorbed in many cases is so low that the data become less accurate.

From Eq.(3.21), $V_m = 1/(S+1)$, where S is the slope and is equal to $(C-1)/V_mC$ and I is the intercept and is equal to $1/V_mC$. This proceeds from the fact that

$$S + I = \frac{1}{V_m C}[(C-1)+1] = \frac{1}{V_m} \qquad (3.23)$$

The surface of the catalyst may then be calculated from V_m if the average area occupied by an adsorbed molecule is known.

Any condensable inert vapor can be used in the **BET** method, but for the most reliable measurements, the molecules should be small and approximately spherical. The vapor also should be easy to handle at the required temperatures; for example , P/P_o values of 0.05 to 0.3 should be conveniently attainable. Krypton, argon and nitrogen are suitable choices in view of their commercial availability. Liquid nitrogen is a readily available coolant, but argon and krypton are expensive relative to nitrogen and must be highly purified. Consequently, nitrogen is usually used since it is relatively cheap and readily available in high purity. It yields well-defined type II curves on most surfaces, and the cross-sectional area per adsorbed molecule has been well established.

The partial pressures of nitrogen gas will be in the range of 10 to 100 kPa in order to obtain values of P/P_o in the range of about 0.05 to 0.30. When the total

surface area of the sample is less than a few square meters, the amounts of gas adsorbed become small relative to the total amount in the apparatus and the accuracy of the measurements becomes poor. By using a vapor of higher boiling point as an adsorbate, measurements at the temperature of liquid nitrogen can be made at much lower pressures to achieve the desired range of P/P_o values; so the amount of gas adsorbed on the solid is now a much larger fraction of that present and can be more precisely measured. The gas most often used for such low-pressure measurements is krypton, which has a vapor pressure at this temperature of about 0.4 kPa. However, the experimental difficulties with low-pressure equipment are somewhat greater because the system must be completely leakproof.

With any adsorbate it is desirable to desorb water and other gases from the vessels and from the sample, typically by heating under vacuum, before making the measurements. If this is not done, slow desorption during determination of the isotherm can give misleading results. Measurements can be made either gravimetrically or volumetrically, and a variety of types of apparatus have been designed and used. In a representative procedure the sample is first degassed at 180 to 190°C for 10 to 15 minutes under vacuum. It is then cooled to liquid-nitrogen temperature, and a known quantity of nitrogen gas is then admitted and allowed to equilibrate. From the equilibrium pressure and *PVT* relationships the amount of nitrogen adsorbed is calculated. The procedure is repeated, yielding a series of values of the volume adsorbed corresponding to a set of increasing values of the equilibrium pressure.

The projected cross-sectional area of an adsorbed gas molecule, A_m can be estimated from the liquid density, but there is no assurance that the packing in a monolayer will be the same as that in the bulk. Thus, for accuracy the method has to be standardized by measurements with adsorbents whose area can be determined directly, e.g., nonporous, finely divided, uniform crystals or spheres. By this means the value for nitrogen has been established as 0.134 nm^2, which, perhaps coincidentally, equals that calculated from the bulk density.

If the constant C is sufficiently large, for example, greater than about 50 (dimensionless), as it usually is with nitrogen adsorption, the isotherm should have a well-defined point B and the intercept is usually small relative to the slope. Hence a straight line can be drawn connecting the origin and one point obtained at a P/P_o value of about 0.2 to 0.3 to obtain the slope for the BET equation. This is a simple, quick method requiring only one datum point, which is very useful for a surface of known properties. The calculation are frequently in error by only a few percents.

The use of one fixed value for the effective cross-sectional area of an adsorbed gas molecule assumes that this is unaffected by the nature of the solid. For most adsorbates on most solids the effective value of A_m varies somewhat from solid to solid because the lattice parameter of the solid causes some localization of the adsorption, i.e., preferential adsorption on certain sites. Hence, a very strongly adsorbed vapor, which corresponds to a high C value, is not desired, but a weakly adsorbed vapor is likewise not desired because of the loss in accuracy in determining the amount of adsorption corresponding to a monolayer. Nitrogen is unusual in that it produces a well-defined knee on most solids, but its adsorption is not excessively localized. Water vapor is not recommended for general use because it has a variety of specific interactions with oxide structures commonly encountered in catalysis and its tends to form an organized tetrahedral structure rather than a random orientation.

The theory underlying the BET model has been criticized for the fact that it postulates that adsorption can occur in the n*th* layer before the (n-1)*th* layer is filled. This implies that molecules can be piled up on top of one another into a system of irregular vertical columns, whereas surface energy considerations indicate that there is probably little adsorption onto the n*th* layer until the (n-1)*th* layer is largely filled. For this and other reasons the constant C should be treated as an empirical parameter rather than a quantity that can be calculated independently. Modifications to the BET model to bring it closer to reality, however, do not change the calculated surface area

appreciably from that obtained from the simple theory, probably in part because multilayer adsorption is not great over the P/P_o range usually used for BET area measurements.

A variety of other equations can also be used, but they seem to offer no significant advantage over the BET method. If much of the area is in the form of pores with diameters less than say 1 to 1.5 nm or so, as occurs with some activated carbons and zeolites, pore condensation may occur at relatively low values of P/P_o, and reported BET areas may be misleadingly high. The highest surface areas reliably obtained for porous substances are about 1000 to 1200 m^2/g, and values reported much higher than this range should be examined critically. The proceedings of an international symposium on surface-area determination critically compared and contrasted various methods.

3.6 Pore-size distribution (Satterfield, 1980)

This is of interest primarily for prediction of the effective diffusivity in a porous catalyst in conjunction with calculations of the ease of access of reactant molecules to the interior of a catalyst pellet by diffusion. Two different methods may be used physical adsorption of a gas, which is appreciable to pores less than about 60 nm in diameter, and mercury porosimetry, applicable to pores larger than about 3.5 nm. The true pore structure is of almost infinite complexity, and a considerable literature exists on interpretation, in terms of pore shapes, of hysteresis loops from physical adsorption data and, to a lesser extent, from mercury porosimeter results.

The pore-size distribution reported depends upon the model assumed for interpretation, This is usually taken as an array of cylindrical capillaries of different radii, randomly oriented. If the pores are fairly close in size, a useful concept is that of the average pore radius defined as $r = 2\ V_g/S_g$, where V_g is the pore volume per gram and S_g the surface area per gram; for example, r is the radius of a cylinder having the

same volume/surface ratio as the real pore. If the pores vary substantially in size, the diffusion characteristics in the structure cannot be adequately represented by an average radius, and it is necessary to determine the pore-size distribution.

Pores lager than about 50 nm in diameter are generally termed macropores; those less than about 2 nm, micropores; and pores of intermediate size, mesopores.